JACS
JOURNAL OF THE AMERICAN CHEMICAL SOCIETY

Communication

pubs.acs.org/JACS

A Small-Molecule Photoactivatable Optical Sensor of Transmembrane Potential

Vincent Grenier,[†] Alison S. Walker,[†] and Evan W. Miller*[,†,‡,§]

Departments of [†]Chemistry, [‡]Molecular & Cell Biology, and [§]Helen Wills Neuroscience Institute, University of California, Berkeley, California 94720, United States

Supporting Information

ABSTRACT: This paper discloses the design, synthesis, and imaging applications of the first member of a new class of SPOTs, small-molecule photoactivatable optical sensors of transmembrane potential. SPOT2.1.Cl features an established voltage-sensitive dye, VoltageFluor2.1.Cl—or VF—capped with a dimethoxy-*o*-nitrobenzyl (DMNB) caging group to effectively diminish fluorescence of the VF dye prior to uncaging. SPOT2.1.Cl localizes to cell membranes and displays weak fluorescence until photoactivated. Illumination generates the parent VF dye which then optically reports on changes in the membrane voltage. After photoactivation with spatially restricted light, SPOT2.1.Cl-loaded cells display bright, voltage-sensitive fluorescence associated with the plasma membrane, while neighboring cells remain dark. Activated SPOT reports on action potentials in single trials. SPOT can be activated in neuron cell bodies or uncaged in dendrites to enable structural tracing via "backfilling" of the dye to the soma, followed by functional imaging in the labeled cell. The combination of cellular specificity achieved through spatially defined patterns of illumination, coupled with the fast, sensitive, and noncapacitive voltage sensing characteristics of VF dyes makes SPOT2.1.Cl a useful tool for interrogating both structure and function of neuronal systems.

Changes in neuronal membrane potential encode the vast range of thoughts, feelings, and behaviors that comprise the human experience. Despite the central importance of the brain to human health and disease, the molecular and cellular mechanisms underlying brain and neuronal function remain incompletely characterized, prompting efforts at the national and international level to develop more comprehensive maps of neuronal activity.[1−3] Much of modern neurobiology stands upon the electrophysiological recordings of the activity of single neurons embedded within a network context. While this approach has proven incredibly powerful, real limitations exist. Specifically, the invasive requirement of impaling cells with electrodes in biological samples severely disrupts overlying tissue and restricts recordings to the cellular soma, making multisite recording challenging or impossible.

Fluorescence imaging uniquely addresses this problem because the technique is noninvasive, can provide spatial information on membrane potential changes in multiple cells or in subcellular regions distant from the soma, and can be high-throughput. Voltage imaging with autofluorescent proteins,[4−7] small molecules,[8−13] or a combination of both[14−16] remains an attractive solution because it can enable the direct measurement of membrane potential while providing the spatial resolution, throughput, and parallel recording capabilities of Ca^{2+} imaging approaches. Recently, voltage-sensitive small molecules based on molecular wires emerged as an intriguing class of fluorophores for voltage sensing.[17,18]

VoltageFluors, or VF dyes, sense changes in transmembrane potential by a photoinduced electron transfer (PeT) mechanism. PeT from an electron-rich aniline through a molecular wire to a fluorescent reporter is controlled by the electric field across the plasma membrane of an excitable cell, such as a neuron. At rest, where typical mammalian neuronal membrane potentials are approximately −60 mV inside the cell, PeT is enhanced, resulting in diminished fluorescence. As the membrane depolarizes—during an action potential or upon integration of excitatory inputs from connected neurons—PeT decreases, resulting in enhanced fluorescence. Consequently, VF dyes display large voltage-sensitive change in fluorescence while maintaining the fast response time needed for resolving single action potential spikes. Because PeT within the VF dye scaffold is fast compared to the biological event of interest, VF dyes add no capacitive load, making them ideal candidates for nondisruptive sensors of neuronal activity.

Despite these important characteristics, the amphipathic nature of VF dyes results in nonspecific uptake into all plasma membranes within a biological sample, obscuring the boundary between adjacent stained cells and making it difficult to detect voltage-induced fluorescence changes against a high background of nonexcitable cells stained with the dye. The ability to sparsely label neurons with VF dyes would address this problem. Restricted labeling of a subset of neurons within a neuronal network would improve signal-to-noise by lowering background fluorescence and pave the way for optical interrogation of local neuronal circuits both in culture and in more complex preparations. To achieve selective labeling of only a fraction of defined neurons, we envisioned quenching VF fluorescence with a photolabile protecting group (Scheme 1).

Photolabile protecting groups have found broad utility in both organic synthesis and chemical biology. Originally developed as a protecting group for amino acids that could be removed under mild conditions, the *o*-nitrobenzyl protection group and its derivatives have since found broad utility in masking the

Received: May 29, 2015
Published: August 6, 2015

DOI: 10.1021/jacs.5b05538
J. Am. Chem. Soc. 2015, 137, 10894−10897

Scheme 1. Synthesis and Photoactivation of SPOT

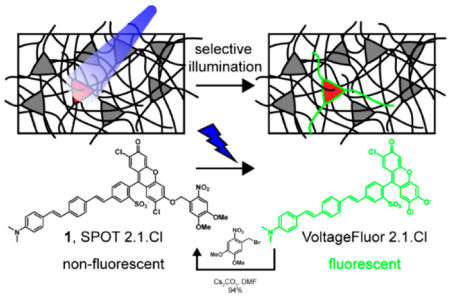

physiological activity of biologically active molecules, including nucleotides, metal ion ligands and ionophores, neurotransmitters, reactive oxygen species, receptor agonists, and amino acid residues. Nitrobenzyl motifs have also been applied to fluorophores for superresolution microscopy. We propose to use photoactivatable VF dyes based on DMNB photocages to spatially control the apparent staining of cells in biological samples. The caged VoltageFluor would localize to cell membranes and remain weakly fluorescent until uncaging or photoactivation via illumination liberated the parent VF fluorophores (Scheme 1). Restricting uncaging illumination by scanning a region of interest (ROI) or through spatial light modulation (SLM) technology would provide targeted fluorescent labeling of defined subpopulations of neurons. Toward this end, we now present the design, synthesis, and application of a **s**mall-molecule **p**hotoactivatable **o**ptical sensor of **t**ransmembrane potential, or SPOT (compound **1**), as a first class of voltage sensing fluorophores that enable targeted photoactivation of VF dyes in cells of interest via selective photoactivation.

SPOT2.1.Cl is readily available in one step from previously reported VF compounds.[17,18] Alkylation of VF2.1.Cl with 2-nitro-4,5-dimethoxybenzyl bromide in DMF provides SPOT2.1.Cl in 94% yield (Scheme 1). We examined the photophysical behavior and characteristics of SPOT2.1.Cl under simulated physiological conditions (PBS, pH 7.4). As synthesized, SPOT2.1.Cl displays an absorbance profile significantly altered from the parent VF dye (SI Figure 1a, gray and black traces), with a λ_{max} centered at 400 nm (ε = 44 000 M^{-1} cm^{-1}) attributed to the molecular wire absorbance and a minor absorbance centered at 500 nm (ε = 21 000 M^{-1} cm^{-1}) corresponding to the alkylated fluorescein scaffold. At 522 nm, the λ_{max} for VF2.1.Cl, SPOT2.1.Cl shows only weak absorbance (ε = 6200 M^{-1} cm^{-1}). In contrast, the free VF dye demonstrates strong absorbance at 522 nm, with a shoulder at 488 nm. Emission from SPOT2.1.Cl is minimal (Figure 1a, black trace), as reflected by its low fluorescence quantum yield (Φ = 0.002), which is 28-fold lower than VF dye (Φ = 0.057). UV illumination of SPOT2.1.Cl promptly delivers VF2.1.Cl, as measured by complete recovery of absorbance profiles characteristic of VF2.1.Cl (SI Figure 1a, green and black traces) and a 25-fold increase in fluorescence emission (Figure 1a, green trace). HPLC comparison against VF2.1.Cl confirmed the photochemical conversion of SPOT2.1.Cl into VF2.1.Cl (SI Figure 2). Identical UV irradiation had no effect on VF2.1.Cl absorbance or emission (SI Figure 1b and c). The photochemical quantum yield was determined by actinometry to be 0.007. SPOT has an ε_{365} of 33 000 M^{-1} cm^{-1} giving an overall efficiency ($\Phi \times \varepsilon_{365\ nm}$) of 230, comparable to reported values for *o*-nitro photocages.

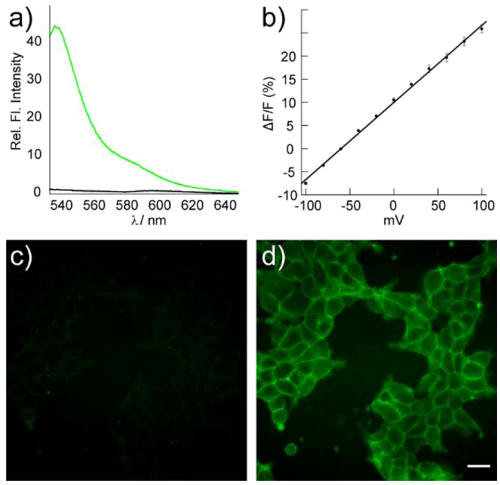

Figure 1. Characterization of SPOT2.1.Cl. (a) Emission spectra of SPOT2.1.Cl in PBS, pH 7.4, before (black trace) and after (green trace) illumination at 365 nm (λ_{ex} = 522 nm). (b) Plot of $\Delta F/F$ vs mV for SPOT2.1.Cl after photoactivation in HEK cells. Error bars are ±SEM for n = 9 experiments. (c) HEK cells loaded with 500 nM SPOT2.1.Cl prior to illumination. (d) Cells from panel (c) after illumination with 390 nm light for 30 s. Scale bar is 20 μm.

We next turned our attention to photoactivation of SPOT2.1.Cl in living cells. Bath application of SPOT2.1.Cl to human embryonic kidney cells (HEK 293) resulted in very little cellular fluorescence staining, due to the low intrinsic brightness of SPOT2.1.Cl (Figure 1c). Illumination with 390 nm (30 × 1 s) light resulted in an immediate increase in cell membrane-associated fluorescence characteristic of VF staining (Figure 1d) over the entire field, indicating that SPOT2.1.Cl had localized to cell membranes and remained optically silent until photoactivation. Quantification of the mean cellular fluorescence intensity pre- and post-UV indicates that SPOT2.1.Cl provides a 12 ± 1.2-fold (n = 3 separate experiments) increase in fluorescence intensity following irradiation. Membrane-associated fluorescence depends on prior UV illumination, as examination of fields of view not exposed to light show little fluorescence (SI Figure 3a, c, e). However, subsequent photoactivation of these regions (390 nm, 30 s) results in a similar fluorescence increase (SI Figure 3b, d, f), demonstrating that patterns of spatially restricted light can selectively photoactivate distinct cell populations.

Having established the ability of SPOT2.1.Cl photoactivation to control apparent staining at a region-specific level, we next examined the ability of SPOT2.1.Cl to label individual cells, using confocal microscopy. By defining a photoactivation ROI around several cells, SPOT2.1.Cl could be selectively activated in the cells of interest (SI Figure 4a and b), giving an approximately11-fold increase (±0.8, n = 5 cells, SI Figure 4d) in fluorescence intensity in cells illuminated with 405 nm light (25 × 1 s illumination, SI Figure 4a–c). Upon release by light, SPOT2.1.Cl remained localized in single cells; the dye did not migrate away from the originally uncaged cells (SI Figure 4b). Uncaged SPOT2.1.Cl, however, freely diffuses within cell membranes. Confocal imaging of HEK cells loaded with SPOT2.1.Cl show minimal fluorescence prior to photoactivation, as before (Figure 2a). Photoactivation of one-half of a HEK cell (yellow area, Figure 2a) delivered a prompt increase in VF2.1.Cl fluorescence in the illuminated half of the cell (Figure 2b). After 10 min, the rest of the cell "fills" with dye, as photoactivated SPOT2.1.Cl diffuses laterally through the

DOI: 10.1021/jacs.5b05538
J. Am. Chem. Soc. 2015, 137, 10894–10897

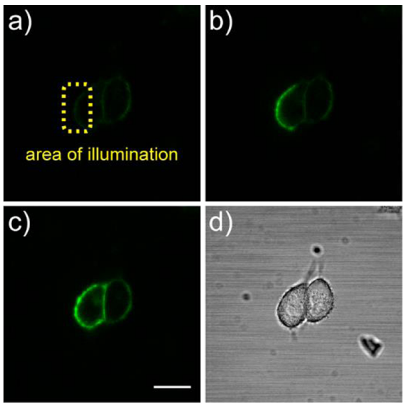

Figure 2. Photoactivation of SPOT2.1.Cl within a single cell. HEK cells loaded with 500 nM SPOT2.1.Cl (a) prior to and (b) immediately after uncaging in an area over the left side of the cell, as indicated by the yellow region of interest in panel (a). Initially, fluorescence fills only the uncaged portion of the cell (b), but after 10 min, (c) the entire cell membrane appears fluorescent, while the neighboring cell remains dim. (d) Transmitted light image of cells in previous panels. Scale bar is 20 μm.

plasma membrane (Figure 2c). The neighboring cell (Figure 2d) remains darker (Figure 2b and c) and shows minimal fluorescence increase. Directly uncaged regions increase fluorescence by 520% (±60%) while neighboring regions increase fluorescence by only 40% (±17%, SEM for n = 4 experiments, SI Figure 5). Diffusion of SPOT away from the uncaging site in confluent monolayers is minimal (SI Figure 6), and VF2.1.Cl behaves nearly identically to the canonical lipophilic tracer dye, DiO, in FRAP experiments in confluent monolayers of HEK cells (SI Figure 7). Taken together, these experiments establish that uncaged SPOT diffuses rapidly within cells, but much more slowly across plasma membranes, in a manner similar to DiO.

Following illumination, cells stained with SPOT2.1.Cl become bright and voltage-sensitive. Whole-cell patch clamp electrophysiological measurements in HEK cells reveal that postillumination, activated SPOT2.1.Cl has a voltage sensitivity of 17% $\Delta F/F$ per 100 mV (Figure 1b and SI Figure 8d), approximately 77% of the sensitivity achieved by the parent VF2.1.Cl under similar recording conditions (SI Figure 8d and e). This decrease in voltage sensitivity may arise from improper membrane orientation of SPOT prior to uncaging[17,18] or photochemically initiated side reactions not observed *in vitro*, and experiments are underway to determine the genesis of this effect. The small decrease in voltage sensitivity does not prevent optical recording of physiologically relevant voltage changes. Whole-field uncaging of cultured neurons loaded with SPOT2.1.Cl, followed by field stimulation, demonstrated that activated SPOT can optically record action potentials in single trials (SI Figure 9). Photolysis of SPOT2.1.Cl is well-tolerated by both HEK cells and neurons, as judged by analysis of MTT viability assays (SI Figure 10) and electrophysiological parameters of HEK cells treated with SPOT2.1.Cl+UV light (SI Figure 11a–e). Neurons loaded with either SPOT2.1.Cl+UV or VF2.1.Cl show no difference in action potential duration (SI Figure 11f)

We envisioned that SPOT2.1.Cl could find utility in complex neuronal contexts wherein optically orthogonal fluorescent proteins targeted to genetic subsets of neurons guide spatially resolved photoactivation of SPOT2.1.Cl and enable sparse labeling and optical recording in neurons. We cultured rat hippocampal neurons (E18) for 14 days *in vitro* (DIV) and transfected them with mCherry localized to the inner leaflet of the cell membrane via a CAAX-mediated farnesylation sequence. A small percentage of neurons displayed good expression of farnesylated mCherry (Figure 3a and b). These neurons were targeted for uncaging by restricting the uncaging region to a <20 μm diameter photoactivation spot centered within the soma defined by mCherry fluorescence (Figure 3b and d). Photoactivation yielded bright membrane-localized fluorescence (Figure 3c, e, and f). Photoactivated SPOT2.1.Cl in neurons reports on action potentials evoked by field stimulation (Figure 3g) with a response of 9% $\Delta F/F$ per action potential (±0.2%, n = 29 APs from 3 cells) and an SNR of 14 ± 4 to 1 (n = 29 APs from 3 cells).

Precise identification of neuronal pathways and function are critical for dissecting connectivity and information processing in the brain. Current neuronal tracing methods rely on diffusion of lipophilic carbocyanine fluorescent tracers and typically require invasive local delivery of dye via pipet. These tracers, while providing a structural description of neuronal projections, cannot report on the activity of labeled neurons. We envisioned that SPOT2.1.Cl, as a voltage-sensitive dye that diffuses within membranes, could be exploited to map local circuitry. By uncaging SPOT2.1.Cl in cellular processes and allowing diffusion of the dye to the soma, cells which were "wired" into the photoactivated region would become bright, allowing imaging of neuronal activity in the labeled cells.

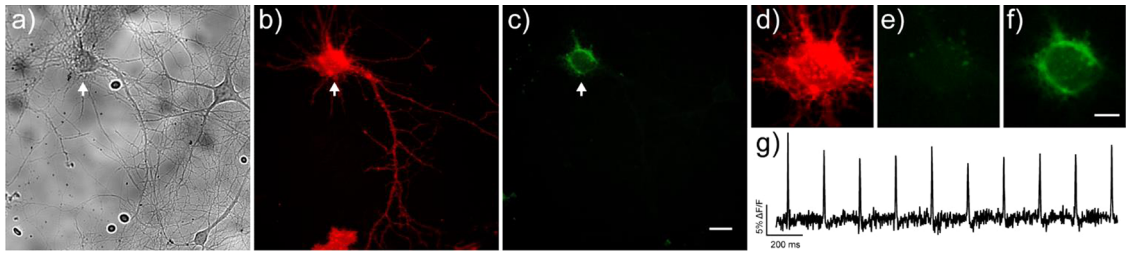

Figure 3. SPOT2.1.Cl uncaging in single neurons. Dissociated, cultured rat neurons (a) were transiently transfected with CAAX-mCherry for use as a fiducial marker for illumination. Panels (a) and (b) show DIC and mCherry fluorescence images, respectively. Cells were loaded with 500 nM SPOT2.1.Cl and then photoactivated (390 nm, 10 s, 22.3 W/cm^2) over a region defined by the somatic staining of the mCherry signal (white arrow). (c) Following photoactivation, VF fluorescence appears to be membrane-localized. (d–f) EMCCD image of indicated cell, showing mCherry fluorescence. VF dye fluorescence from the mCherry-positive neuron, (e) prior to SPOT2.1.Cl photoactivation and (f) immediately after. (g) Field stimulation of the SPOT2.1.Cl-stained neuron at 5 Hz produced a train of optically recorded action potentials, which were captured in a single trial at 500 Hz with an EMCCD camera. Scale bars are 20 μm for panels a–c and 10 μm for panels d–f.

DOI: 10.1021/jacs.5b05538
J. Am. Chem. Soc. 2015, 137, 10894–10897

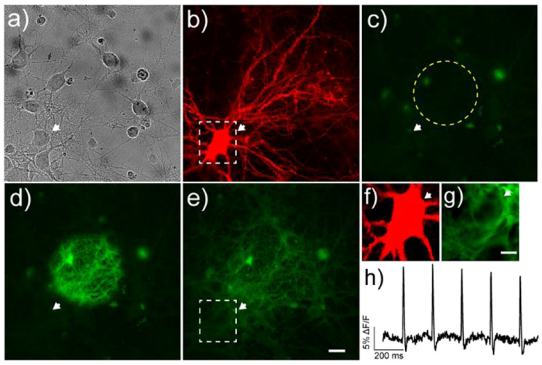

Figure 4. Voltage sensing in neurons identified by SPOT retrograde tracing. Neurons were stained with 2.5 μM SPOT2.1.Cl. (a) DIC image of neurons stained with SPOT2.1.Cl. b) Widefield epifluorescence image of neurons in panel (a), demonstrating labeling with mCherry-CAAX. (c) Green fluorescence image of same cells, prior to SPOT2.1.Cl photoactivation. Area of photoactivation is indicated by yellow dotted circle. (d) Cells in panel (c) immediately after photoactivation. (e) Diffusion of photoactivated SPOT2.1.Cl away from uncaging area after 30 min at 37 °C. (f) mCherry-positive neuron from panel (b) within the region in dotted white box. (g) Image of SPOT2.1.Cl-traced neuron used to generate functional imaging data, after photoactivation and diffusion. (h) Action potentials evoked by field stimulation of neurons at 5 Hz and recorded optically in the indicated cell—white arrow—in a single trial at 500 Hz. Scale bar is 20 μm (a–e) and 10 μm (f and g).

To explore this, we first ascertained the ability of photoactivated SPOT2.1.Cl to diffuse within neuronal membranes. Indeed, neurons loaded with SPOT2.1.Cl and uncaged in the soma showed substantial diffusion of activated SPOT2.1.Cl away from the soma into distal processes when the neurons were maintained at 37 °C (SI Figures 12 and 13). We then loaded cultured hippocampal neurons expressing cell membrane-localized mCherry (Figure 4a and b) with SPOT2.1.Cl and photoactivated a region (Figure 4c, yellow circle) lacking cell bodies, but containing numerous processes, including those of an mCherry-positive cell. Following uncaging, we maintained the neurons at 37 °C to allow activated SPOT2.1.Cl to diffuse back toward cell bodies that projected processes into the uncaging region. After 30 min, several cell bodies were highlighted (Figure 4e), including the mCherry-positive cell, indicating that SPOT2.1.Cl can be used to map local connectivity in living neurons. Upon field stimulation, uncaged SPOT2.1.Cl clearly distinguishes action potentials in single trials from neurons labeled by retrograde tracing (Figure 4g and h), demonstrating that SPOT methodology can be used to report both structural and functional connectivity and dynamics within local circuits, which cannot be achieved with VF or lipophilic tracer dyes in isolation.

In summary, we present the design, synthesis, and biological evaluation of the first member of a new class of voltage sensitive dyes—SPOTs, small photoactivatable optical sensors of transmembrane potential. In particular, SPOT2.1.Cl, based on the VoltageFluor2.1.Cl scaffold, exhibits a large fluorescence dynamic range following near-UV photoactivation, good voltage sensitivity, staining defined by spatially restricted illumination and enables functional imaging of genetically specified neurons through an optically orthogonal marker, either through direct photoactivation of cells of interest or via "backfilling" in which neuronal processes are uncaged to provide labeling in cell bodies. Current efforts are underway in our lab to apply SPOT2.1.Cl to brain tissue, as well as to explore new photocaging scaffolds with increased two-photon uncaging cross-section, improved water solubility, and enhanced targeting and retention in membranes.

■ ASSOCIATED CONTENT

Supporting Information

The Supporting Information is available free of charge on the ACS Publications website at DOI: 10.1021/jacs.5b05538.

Synthetic methods, imaging parameters, cell culture conditions, additional references (PDF)

■ AUTHOR INFORMATION

Corresponding Author

*evanwmiller@berkeley.edu

Notes

The authors declare no competing financial interest.

■ ACKNOWLEDGMENTS

This work was generously supported by start-up funds from the University of California and the NIH (R00NS078561). V.G. was supported in part by a fellowship from NSERC. Confocal microscopy was performed at the Molecular Imaging Center at UC Berkeley.

■ REFERENCES

(1) Alivisatos, A. P.; Chun, M. Y.; Church, G. M.; Greenspan, R. J.; Roukes, M. L.; Yuste, R. *Neuron* **2012**, *74*, 970.
(2) Insel, T. R.; Landis, S. C.; Collins, F. S. *Science* **2013**, *340*, 687.
(3) Alivisatos, A. P.; Chun, M.; Church, G. M.; Deisseroth, K.; Donoghue, J. P.; Greenspan, R. J.; McEuen, P. L.; Roukes, M. L.; Sejnowski, T. J.; Weiss, P. S.; Yuste, R. *Science* **2013**, *339*, 1284.
(4) Jin, L.; Han, Z.; Platisa, J.; Wooltorton, J. R.; Cohen, L. B.; Pieribone, V. A. *Neuron* **2012**, *75*, 779.
(5) Akemann, W.; Sasaki, M.; Mutoh, H.; Imamura, T.; Honkura, N.; Knopfel, T. *Sci. Rep.* **2013**, *3*, 2231.
(6) Hochbaum, D. R.; Zhao, Y.; Farhi, S. L.; Klapoetke, N.; Werley, C. A.; Kapoor, V.; Zou, P.; Kralj, J. M.; Maclaurin, D.; Smedemark-Margulies, N.; Saulnier, J. L.; Boulting, G. L.; Straub, C.; Cho, Y. K.; Melkonian, M.; Wong, G. K.; Harrison, D. J.; Murthy, V. N.; Sabatini, B. L.; Boyden, E. S.; Campbell, R. E.; Cohen, A. E. *Nat. Methods* **2014**, *11*, 825.
(7) St-Pierre, F.; Marshall, J. D.; Yang, Y.; Gong, Y.; Schnitzer, M. J.; Lin, M. Z. *Nat. Neurosci.* **2014**, *17*, 884.
(8) Gonzalez, J. E.; Tsien, R. Y. *Biophys. J.* **1995**, *69*, 1272.
(9) Yan, P.; Acker, C. D.; Zhou, W. L.; Lee, P.; Bollensdorff, C.; Negrean, A.; Lotti, J.; Sacconi, L.; Antic, S. D.; Kohl, P.; Mansvelder, H. D.; Pavone, F. S.; Loew, L. M. *Proc. Natl. Acad. Sci. U. S. A.* **2012**, *109*, 20443.
(10) Fink, A. E.; Bender, K. J.; Trussell, L. O.; Otis, T. S.; DiGregorio, D. A. *PLoS One* **2012**, *7*, e41434.
(11) Bradley, J.; Luo, R.; Otis, T. S.; DiGregorio, D. A. *J. Neurosci.* **2009**, *29*, 9197.
(12) Fromherz, P.; Hubener, G.; Kuhn, B.; Hinner, M. J. *Eur. Biophys. J.* **2008**, *37*, 509.
(13) Fluhler, E.; Burnham, V. G.; Loew, L. M. *Biochemistry* **1985**, *24*, 5749.
(14) Wang, D.; McMahon, S.; Zhang, Z.; Jackson, M. B. *J. Neurophysiol.* **2012**, *108*, 3147.
(15) Sjulson, L.; Miesenbock, G. *J. Neurosci.* **2008**, *28*, 5582.
(16) Chanda, B.; Blunck, R.; Faria, L. C.; Schweizer, F. E.; Mody, I.; Bezanilla, F. *Nat. Neurosci.* **2005**, *8*, 1619.
(17) Miller, E. W.; Lin, J. Y.; Frady, E. P.; Steinbach, P. A.; Kristan, W. B.; Tsien, R. Y. *Proc. Natl. Acad. Sci. U. S. A.* **2012**, *109*, 2114.
(18) Woodford, C. R.; Frady, E. P.; Smith, R. S.; Morey, B.; Canzi, G.; Palida, S. F.; Araneda, R. C.; Kristan, W. B., Jr.; Kubiak, C. P.; Miller, E. W.; Tsien, R. Y. *J. Am. Chem. Soc.* **2015**, *137*, 1817.

DOI: 10.1021/jacs.5b05538
J. Am. Chem. Soc. 2015, 137, 10894–10897